Manoj KUMAR, PhD Scholar
E-mail: manoj1985.111@gmail.com
Department of Electronics and Communication Engineering
Jaypee University of Engineering and Technology Guna, India

Assistant Professor Manish PATIDAR, PhD
E-mail: manish.patidar@juet.ac.in
Department of Electronics and Communication Engineering
Jaypee University of Engineering and Technology Guna, India

Associate Professor Narendra SINGH, PhD
E-mail: narendra.singh@juet.ac.in
Department of Electronics and Communication Engineering
Jaypee University of Engineering and Technology Guna, India

OPTIMIZED MIMO BASED ENHANCED OFDM FOR MULTI CARRIER SYSTEM WITH 5G WAVEFORMS

Abstract. *Orthogonal Frequency Division Multiplexing (OFDM) is a multi-carrier modulation technology that uses many subcarriers inside a single channel to broaden the notion of single subcarrier modulation. Because of its high-power transmission, the above approach produces out-of-band radiation. Therefore, a novel model named MIMO based enhanced OFDM communication system is introduced. In which random data bits are generated by a random data source, which is mapped using QPSK. Furthermore, to alleviate the carrier interference in MIMO-OFDM a novel Multi carrier interference mitigation method is presented. In which the Fourier, ICI estimation is done to separate the signal to time and frequency variant. Therefore, a novel Deep Frequency Time Offset estimation approach is created with two successive layers, and a Deep Neural Network (DNN) is used to estimate the residual carrier frequency offset and symbol timing offset. This reduces the time and frequency offset inaccuracy. Additionally, to alleviate out-of-band problems, a novel Low Complex Equalised demodulating approach is introduced. In which an extension windowing procedure is performed after adding CP, significantly reducing side lobe power and simplifying the process. Thus, the proposed OFDM carriers all the signal and transmits and receives with low out-of-band, carrier frequency offset in an efficient and equalised manner without any error and losses.*

Keywords: *OFDM, Signal detection, Neural networks, Channel estimation, Carrier frequency offset, QPSK*

JEL classification: D83, L96

DOI: 10.24818/18423264/57.2.23.17

1. Introduction

Multimedia-based applications have propelled technical breakthroughs around the world, increasing demand for high-data-rate technologies via wireless and mobile channels (Niu, Zhongqian et al., 2020). However, when the data rate increases, the length of transmitted symbols decreases, resulting in substantial degradation of received symbols due to inter symbol-interference (ISI) caused by dispersive fading in the wireless environment (Shi, Chenguang et al., 2020). This phenomenon is present in single-carrier modulation systems like Time Division Multiple Access (TDMA) and the Global System for Mobile Communications (GSM) (Jiang, Lei et al., 2020). Multiple-input, multiple-output (MIMO) and orthogonal-frequency-division-multiplexing (OFDM) systems have shown promise in addressing the current high data-rate need (Alrubaee, Saif et al., 2020). Because they are orthogonal to one another during one symbol period, subchannels and subcarriers in OFDM can overlap without interfering with one another (Wang, Shi et al., 2021).

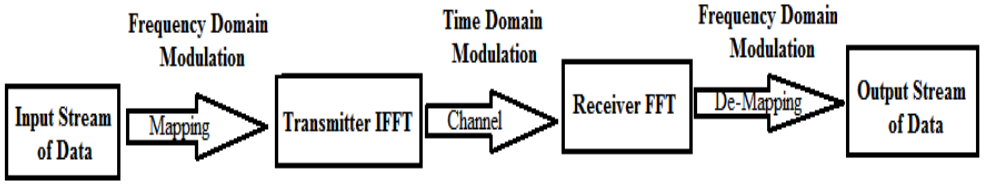

Figure 1. OFDM Modulation and demodulation

Figure 1 demonstrates how parallel data delivery over a number of frequencies in OFDM results in longer information symbol-block intervals than in a serial data-transmission system.

The OFDM system is the focus of many standards and has been extended to fifth-generation networks (Hou, Jun et al., 2020). In order to modulate multiple subcarriers, the input bit stream is divided into several parallel bit streams in MCM (Multi-carrier modulation). The guard band is used to separate the subcarriers in order to prevent them from touching. To separate the spectra of different subcarriers on the receiver side, band-pass filters are used (Shaikhah, Salar Kheder et al., 2020). A spectral efficiency approach known as OFDM uses orthogonal and multispectral interfering spectra. In a field where, single carrier communication was historically the standard, a number of multicarrier (MC) techniques have lately gained popularity (Chen, Qiang et al., 2021). The most well-known is OFDM, which is being investigated in-depth for its ability to combat inter-symbol interference (ISI) and address frequency selectivity in the communication channel at the same time. Due to advancements in next-generation communication technology and their capacity to considerably enhance bandwidth use, a number of evolving multicarrier waveforms have been researched for diverse domains (Srivastava, Mohit Kumar et al., 2020).

The following categories can be used for wireless MCM systems depending on the type of block-transform used. Fast discrete curvelet transform (FDCT)-based systems include those that use the FFT, the modified Lapped transform (MLT), the discrete cosine transforms (DCT), the wavelet transforms (WT), and the fast discrete curvelet transform (FDCT) (Attar, Hani et al., 2020). The five different forms of WT-based systems include discrete wavelet transform (DWT), wavelet packet transform (WPT), complex wavelet packet transform (CWPT), and dual-tree complex wavelet transform (DTCWT) systems (Murad, Mohsin et al., 2020).

As a result, it creates a challenge for the development of 5G communication networks with high data rates (Ahmed, Saadaldeen Rashid et al., 2020; Alrubaee, Saif et al., 2020). It requires a vast flow of data in the form of audio/video content. A successful method for enabling high data-rate/capacity wireless systems without sacrificing performance has been found to be the combination of spatial-coding methods and multicarrier transmission. As a potential candidate for multicarrier communication, orthogonal-frequency-division-multiplexing (OFDM) technology has been identified (Mattera, David et al., 2021). Its defining characteristic is the ability of OFDM to split the allotted bandwidth into a number of orthogonal narrowband subchannels (overlapping), which turns a frequency-selective channel into a collection of frequency-nonselective flat-fading subchannels.

Furthermore, the OFDM communication system offers simple Frequency Domain Equalisation (FDE) and strong inter-Symbol-Interference mitigation (ISI) (Shaikhah, Salar Kheder et al., 2020). The OFDM communication system, on the other hand, suffers from two sources of performance degradation: the receiver's sensitivity to Carrier Frequency Offset (CFO) and the transmitter's huge Peak-to-Average Power Ratio (PAPR).

The contribution of this paper,

- A **MIMO-based enhanced OFDM communication system** is presented to govern which random data bits are generated by a random data source using quadrature phase shift keying.
- A **Multicarrier interference mitigation** approach is introduced to isolate the signal from the time and frequency variants in ICI estimation.
- The residual symbol timing offset and residual carrier frequency offset are estimated with the aid of a Deep Neural Network (DNN) using **Deep Frequency Time Offset estimation method.**
- Low Complex Equalised demodulating approach were introduced in which an extension windowing process is done after adding CP which highly reduces the power of side lobe and lowers the complexity.

The paper is divided into five sections: section 2 contains recent literatures, section 3 depicts a detailed description of the suggested approach, section 4 analyses the implementation outcomes, and section 5 ends the paper.

2. Literature Survey

Attar, Hani et al. (2020) created a low complexity band LDLH factorisation equaliser for mobile medical communication systems. Additionally, the discrete fractional Fourier transform (DFrFT) is used to improve the efficiency of the communication system using OFDM. The performance of OFDM and DFrFT-orthogonal chirp division multiplexing (DFrFT-OCDM) systems may be enhanced by the proposed low-complexity equaliser. The performance of the MCM system under doubly dispersive fading channels can be improved by the invention of new low-complexity equalisers and alternative bases, although efforts should be made to minimise complexity or power consumption.

Park, Myung Chul et al. (2021) suggested a CNN (Convolutional Neural Network) model based on the fast Fourier transformation window bank (FWB). For extracting the useful symbol length in OFDM, which is needed to identify any OFDM-based wireless communication method. We provide a DL-based system using FWB, in-phase, and quadrature-phase signals to simultaneously classify single-carrier modulation schemes and the useful symbol length of the OFDM. To achieve a high level of classification accuracy in the experiment, the limits of the FWB parameters with respect to the length and FFT size of the OFDM signal are also explored. In the future, OFDM-based signals with shorter input lengths will be needed, as well as new DL (Deep Learning) structures and guard interval estimation.

Sarowa, Sandeep et al. (2020) demonstrated the majority of the traditional and current PAPR reduction solutions, highlighting the possibility for future research in wavelet-based OFDM to create more effective systems using a comparison study and simulative analysis. By integrating wavelet hybridisation, clipping, and companding techniques, PAPR optimisation is made possible. OFDM based on wavelets should be used in conjunction with other PAPR reduction techniques.

Dang, Shuping et al. (2020) proposed an OFDM-SNM method with relay assistance for multi-hop cooperative systems. A relay that uses the decode-and-forward (DF) and half-duplex (HD) protocols must be present at every hop. They examined the outage performance of the relay assisted OFDM-SNM (Subcarrier number modulation) system. The average outage probability is approximated in closed form. Furthermore, in order to show the diversity and coding benefits of relay assisted OFDM-SNM, we employ power series expansion to study asymptotic outage performance at high signal-to-noise ratio (SNR). However, a multi-hop relay cross-layer system architecture was helpful for OFDM-SNM.

Wang, Xiaojie et al. (2020) assessed both effects for cyclic prefix (CP), zero padded (ZP), and universal filtered (UF)-based OFDM with a straightforward one-tap equalisation and the assumption of a doubly dispersive wireless channel model. We demonstrate that, in contrast to perfect examples with a single selectivity, the general channel model's independent (wide sense stationary uncorrelated scatter, WSSUS) selectivity in the time and frequency domain begins to entangle. We get the signal to an interference-plus-noise ratio (SINR) in closed form for various system configurations and channel parameters, such as bandwidth, latency, and

Doppler spread. Using SINR analysis and varied channel conditions, we compare the three MCM approaches. Future work for both waveforms will involve window design and FIR-filter optimisation.

Liu, Xinyue et al. (2020) analysis of the coexistence conditions of orthogonal and non-orthogonal multicarrier signals. Orthogonal frequency division multiplexing (OFDM) and spectrally efficient frequency division multiplexing (SEFDM) signals were the main topics of this analysis. Three main scenarios of coexisting communication with varying subcarrier spacings are covered by 5G New Radio (5G NR) numerology. With the assumption of uncorded and coded signals, this study presents performance findings of systems operating in the investigated coexistence scenarios. The findings demonstrate that systems utilising SEFDM (Spectrally Efficient Frequency Division Multiplexing) and OFDM have some BER loss when employing uncorded signals. The block error rate (BLER) for both orthogonal and non-orthogonal signals, however, only slightly degrades when low-density parity-check (LDPC) is applied to the transmitted signals. This is because the coexistence effects are reduced. It is vital to work on implementing heterogeneous systems that take into consideration 5G NR and non-orthogonal signaling.

The literature review states that Attar, Hani et al. (2020)'s efforts should be made to reduce complexity or power consumption, such as looking for new, low-complexity equalisers and alternative bases that can enhance the MCM system's performance under doubly diffraction fading channels, Park, Myung Chul, et al. (2021) need to adapt other DL structures and the defender interval estimation is necessary for OFDM-based signals with shortened input length, Sarowa, Sandeep, et al., (2020) require to integrate wavelet hybridisation, clipping, and companding techniques in wavelet-based OFDM to achieve a better optimization of Peak-to-average power ratio, Dang, Shuping et al. (2020) need a modulation system with a multi-hop relay cross-layer architecture to improve the performance of OFDM-SNM, Wang, Xiaojie, et al. (2020) need more erudite equalizer with less complex design and optimal combination of FIR-filtering to effectively handle the channel delay spread. Liu, Xinyue, et al., (2020) need to utilize more advanced and refined LDPC coding procedures to eliminate the detrimental impacts of coexisting orthogonal and non-orthogonal signals. A fresh technique must therefore be used to resolve the aforementioned problems.

3. Optimised MIMO based Enhanced OFDM for Multi Carrier System with 5G Waveforms

Multiple subcarriers are used inside of a single channel as part of the multi-carrier modulation technology known as OFDM, which expands the idea of single subcarrier modulation. Because of its high-power transmission, the above approach produces out-of-band radiation. Furthermore, it introduces a new side lobe, lowering the systems channel capacity. To overcome the abovementioned issue, a novel MIMO based enhanced OFDM communication system has been proposed with a

spatial multiplexing. In which a random data source first generates random data bits, which are then mapped via Quadrature Phase Shift Keying (QPSK). Consequently, each stream is modulated using the Inverse Fast Fourier Transform, then inserted with a Cyclic Prefix (CP) to lower the ISI before being sent over a Rayleigh fading channel with six taps based on Jake's model. To mitigate the carrier interference due to various transmitter in MIMO-OFDM a novel multi-carrier interference mitigation method is introduced. In this form of Fourier transform, the signal is separated into time and frequency variants using ICI estimation. Furthermore, to alleviate the time and frequency offset inaccuracy, a unique Deep Frequency Time Offset estimation approach is developed. A Deep Neural Network is used to determine the residual symbol timing offset and residual carrier frequency offset. In addition, this system used a Low Complex Equalised demodulating technique, in which the frequency Domain Equaliser, on the receiver side, interacts with the received signal in the frequency domain and is based on the banded-matrix approximation approach, with no temporal lag.

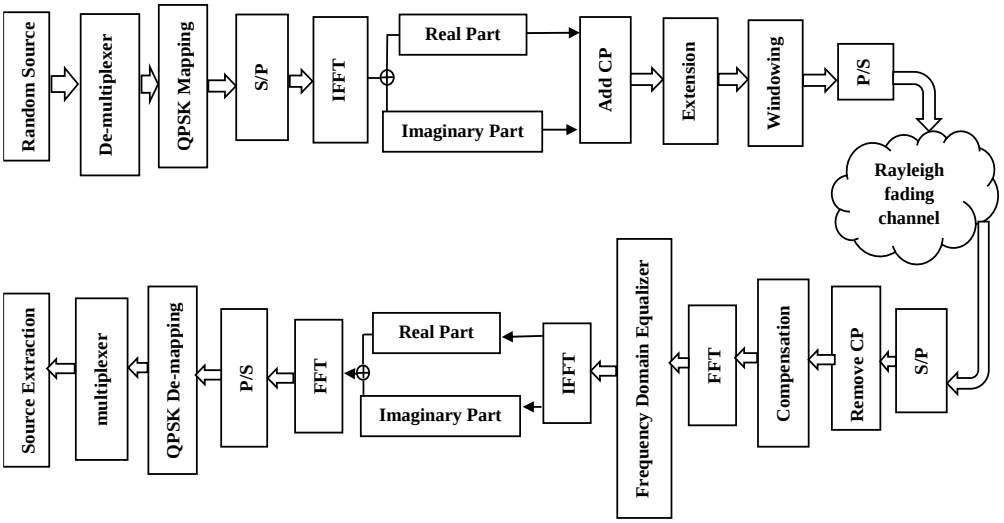

Figure 2. Block architecture of the proposed methodology

As shown in Figure 2, the transmitter and receiver are the two parts of the OFDM communication system. Here, the signal sequence is serial-to-parallel converted, digitally modulated, and pilots are inserted to produce a new sequence at the transmitter. Furthermore, utilising IFFT, the frequency domain signals are translated into time domain signals (Inverse Fast Fourier Transform). In order to prevent ISI, each OFDM frame also carries a cyclic prefix (CP), whose length should be greater than the channel's maximum delay. Time domain data are converted to frequency domain signals once the CP (Cyclic Prefix) has been removed using serial-to-parallel conversion, FFT, and pilots at the receiver for channel estimation.

Additionally, the signal identification and digital demodulation modules work in accordance with the estimated channel, enabling the retrieval of the supplied signal.

3.1. MIMO-based enhanced OFDM for Multi-carrier system

Orthogonal Frequency Division Multiplexing is a technique that is very similar to the widely used Frequency Division Multiplexing (FDM). Moreover, it creates an additional side lobe, which reduces the channel capacity of the system. Hence, to overcome the abovementioned issue a novel **MIMO-based enhanced OFDM for Multi-carrier system** is introduced. In which multiple independent streams are delivered in parallel through multiple antennas and separated at the receiver utilising multiple receive chains and suitable signal processing. Therefore, the number of antennas used in a spatial multiplexing system determines the data rate and capacity increases; for instance, a SM system twice the peak data rate. In addition, the OFDM trans receiver system is designed with a Rayleigh fading channel using QPSK modulation.

The random Integer Generator and Integer to Bit Converter are used as data sources.

- The random bit generator is the initial block in the OFDM system, and it generates the serial binary data that is being sent to the serial to parallel converter.
- The integer number is converted to digital bits using an integer to-bit converter. Each integer or fixed-point value in the input vector is converted to a group of bits in the output vector by the Integer to Bit Converter block. Then, the block converts each integer value to a group of M (total number of subcarrier) bits, with the most significant bit determined by the Output bit order decision. Therefore, the length of the output vector is M times the length of the input vector.

To reduce ISI, the communication takes place across a Rayleigh fading channel. Consequently, the Multipath Rayleigh Fading Channel block simulates a multipath Rayleigh fading propagation channel in baseband. At its input, this block only receives frame-based complex signals. After employing an IFFT to insert pilot tones, the input data symbols are mapped. Through the sending end antennas, the modulated data is sent. Here, FFT is used, and the signal is sent to the carrier sense channel estimation, from which the data symbols are decoded. Moreover, the outputs of the method are transmitted across a noisy channel, and the CP is detached before the FFT (Fast Fourier Transform) technique is used to transform the data. The system standard calls for the addition of a cyclic prefix (cp) to each block of data, and the data is serially multiplexed. Finally, the pilot signal is recorded with the real data signal during the carrier sense channel estimate transmission, and the signal quality is evaluated to determine the actual data signal quality. On the other hand, this

considerably minimises the guard band, enhancing spectral efficiency. Hence, the multicarrier interference mitigation is explained in the following subsection.

3.2. Multi carrier interference mitigation

Inter Carrier Interference (ICI) is caused by the carrier frequency offset violating the orthogonality properties among the sub-carriers. Hence, to overcome the abovementioned issue a novel **MIMO based enhanced OFDM for Multi carrier system.** In which the Fourier, ICI estimation is done to separate the signal to time and frequency variant. So, the ICI components in the time varying channel is estimated and reduced efficiently. Consequently, two separate modulators are used to reduce the computation complexity of real and imaginary signal. When digitally derived binary input data is FEC (Forward Error Correction) coded using convolutional coding methods. The channel coded bits are then collected, transferred to the correct constellation locations, and interleaved with the coded bit stream. At this point, the data are displayed as a series of complex numbers. Add well-known pilot symbols that are associated with established mapping protocols. The IFFT (Inverse Fast Fourier Transform) operation is also carried out on the parallel complex data using a serial to parallel converter. Thereby, the modified data is regrouped according to the number of transmission subcarriers are shown in below equation (1).

The j-th sub-carrier signal after IFFT in the original OFDM is as follows:

$$Y_j = X_j + X_j[Q_0 - 1] + \sum_{\substack{K=0 \\ K\neq j}}^{M-1} X_k\, Q_{k-j} + M_j \tag{1}$$

Where M_j be the jth number of subcarrier

$\sum_{\substack{K=0 \\ K\neq j}}^{M-1} X_k\, Q_{k-j}$ be the Intercarrier Interference signal

on the jth subcarrier, the Y_j be the received intended signal power is

$$[|Y_{j1}|^2 = E[|X_j Q_0|^2] \tag{2}$$

ICI Power,

$$E[|Y_{j2}|^2 = E[\left|\sum_{\substack{K=0 \\ k\neq j}}^{M-1} X_k\, Q_{K-j}\right|^2] \tag{3}$$

After IFFT, the transmitted signal in an OFDM system may be represented as

$$y(n) = \frac{1}{M}\sum_{t=0}^{M-1} Y(t) e^{\frac{j2\pi nt}{M}} \tag{4}$$

where y(n) is the OFDM transmitted signal's nth time domain sample, M is the total number of OFDM subcarriers, Y(t) is the modulated symbol in frequency domain for the tth subcarrier, and $0 \le t \le M-1$ is the total number of OFDM subcarriers.

After passing over the Rayleigh fading channels, the received signal is modified by frequency offset:

$$x(n) = y(n)e^{\frac{j2\pi\varepsilon}{M}} + \omega(n) \quad (5)$$

The normalised frequency offset is calculated as $\Delta f N T_s$, T_s is the symbol period, and f is the frequency variation of the local oscillator between the transmitter and receiver. The AWGN noise introduced into the channel is $\omega(n)$. After performing a frequency domain FFT at the j^{th} subcarrier, the received signal may be represented as

$$X(k) = \sum_{m=0}^{m-1} x(n)e^{\frac{-j2\pi jn}{M}} \quad (6)$$

On the j^{th} subcarrier, $X(k)be$ the received signal can be further represented as,

$$X(k) = Y(k)s(0) + \sum_{\substack{t=0 \\ t\neq j}}^{M-1} x(n)\, s(t-j) + W(j) \quad (7)$$

where, $Y(k)s(0)$ be the desired signal

$\sum_{\substack{t=0 \\ t\neq j}}^{M-1} x(n)\, s(t-j) + W(j)$ be the Inter Carrier Interference signal (ICI)

The intended signal is represented by the right-hand side first term, and the ICI signal for the kth subcarrier is represented by the second term. $W(j)$ is the FFT of $w(n)$, and $s(t-j)$ is the complex ICI coefficient between the tth and kth subcarrier in the received signal. The coefficients are described as follows:

$$s(t-j) = \frac{\sin[\pi(t+\varepsilon-j)]}{M\sin\left[\frac{\pi(t+\varepsilon-j)}{M}\right]} \exp\left[j\pi(t+\varepsilon-j)\left(1-\frac{1}{M}\right)\right] \quad (8)$$

The FFT approach is used to transform the data after the output of the optimised MIMO-OFDM Signal has been transmitted across a noisy channel and the CP has been removed. In addition, the pilot signal is recorded with the real data signal during the carrier sense channel estimate transmission, and the signal quality is evaluated to determine the actual data signal quality. Hence, the deep frequency tie offset estimation method is explained in the below subsection.

3.3. Deep Frequency Time Offset estimation method

A unique Deep Frequency Time Offset estimation approach is provided to reduce the time and frequency offset inaccuracy caused by Sensitive frequency, time synchronisation issues. In this case, a Deep Neural Network (DNN) is employed with two successive layers to estimate the residual symbol timing offset and residual carrier frequency offset, from which the subcarrier location and symbol start point are precisely computed for further processing. The serial OFDM signal's obtained time-domain IQ (In Phase Quadrature) samples are immediately fed into the CFO equalisation network to estimate the signal devoid of CFO effects. After removing the CP, the signal is subsequently transformed into the frequency domain.

Additionally, the channel equalisation network is trained on this frequency domain signal with CFO adjustments in order to analyse the signal without channel effects. Demodulating this signal allows for the subsequent recovery of the sent data.

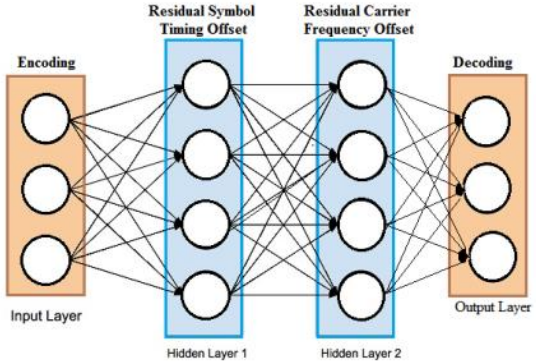

Figure 3. Architecture of the proposed DNN

Figure 3 shows the general architecture of the proposed DNN, which has two successive layers for signal encoding and decoding. Several of these OFDM signals are received in serial to obtain input samples for the DNN, which are given by

$$x[n] = [x_1[n], x_2[n], \ldots . x_{N_f}[n]] \quad (9)$$

where, H is the convolutional layer and N_f is the number of OFDM symbols in a frame,

$$x[n] = Hy_{ch}[n] + w[n] \quad (10)$$

$$H = \frac{e^{j2\pi f(n)n}}{\Delta f_N} \quad (11)$$

$$y_{ch}[n] = y(n) \otimes m[n] \quad (12)$$

As seen in Figure 4, the transmitted OFDM frame x[n], the message signal $m[n]$, the received baseband OFDM signal y(n), and the convolution process $\otimes$ are all denoted.

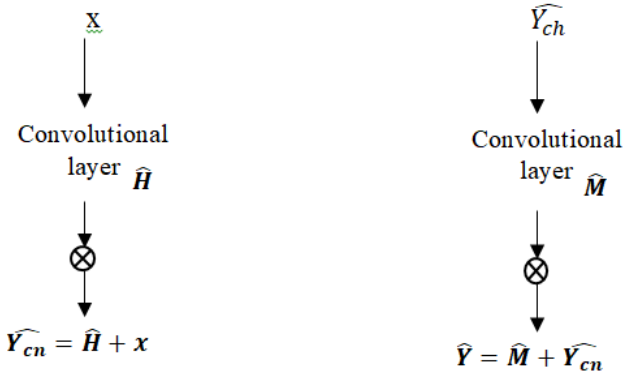

Figure 4. Block figure of CFO and channel equalisation

The CFO equalisation network receives the received baseband signal y(n) or $\widehat{y_{ch}}[n]$. Now, if the output of the CFO equalisation networks before the skip connection is $y_{ch}[n]$, the input may be expressed as

$$\mathrm{y_{ch}[n]} = \widehat{\mathrm{H}} * (\mathrm{Hy_{ch}[n]} * \mathrm{w[n]}) \tag{13}$$

The following equation may be expressed as if the influence of AWGN (Additive white Gaussian noise) is disregarded.

$$\widehat{\mathrm{y_{ch}}}[\mathrm{n}] = \widehat{\mathrm{H}} * \mathrm{Hy_{ch}[n]} + \mathrm{w[n]} \tag{14}$$

To counteract the effects of CFO, the projected $\widehat{H}$ value must be closer to the complex conjugate of H .As a result, the network is trained to attain the lowest mean-squared error cost function.

$$\mathrm{E_{CFO}} = (\widehat{\mathrm{y_{ch}}}[\mathrm{n}] - \mathrm{y_{ch}[n]})^2 \tag{15}$$

After removing the CP and taking the FFT of the output signal from the CFO equalisation network, the CFO (Carrier frequency offset) corrected frequency domain signal is obtained.

$$\widehat{\mathrm{Y_{ch}}}[\mathrm{j}] = \mathrm{FFT}(\widehat{\mathrm{y_{ch}}}[\mathrm{n}]) = \mathrm{Y[j]M[j]} \tag{16}$$

where: $M[j]$ is the channels frequency domain response.

$Y[j]$ be the estimated channel equalised signal.

$$\mathrm{Y[j]} = \widehat{\mathrm{H}}[\mathrm{j}] * (\mathrm{Y[j]M[j]}) \tag{17}$$

In order to learn the estimate $\widehat{H}$, whose value should be near to the inverse of the genuine channel response, the cost function is reduced in the channel equalisation network during training.

$$\mathrm{E_{chan}} = (\widehat{\mathrm{Y}}[\mathrm{j}] - \mathrm{Y[j]})^2 \tag{18}$$

Additionally, the bit error rate is calculated after demodulating the predicted signal $\hat{Y}[j]$. Also, the use of a deep learning algorithm yields successful performance without the use of perfect CSI or prohibitive processing complexity.

3.4. Low Complex Equalised demodulating approach

To alleviate out-of-band issues, the system uses a low-complexity equalised demodulating technique, which involves performing an extension windowing operation after adding CP, drastically decreasing side-lobe power, and simplifying the system. As a result of the channel delay while sending the OFDM symbol, ISI occurs at the receiver. The guard interval is added in between the succeeding OFDM signals to prevent the ISI. Additionally, a sufficient guard interval is constructed regarding the channel's delay spread, and the cyclic prefix is provided to the guard interval to circumvent ISI. The fundamentals of CP are outlined below.

Interference between OFDM symbols can be minimised by using zeros in the guard time. The carriers' orthogonality is lost when multipath channels are used, though CP can bring it back. In addition, the cyclic prefix converts the linear

convolution channel to a circular convolution channel, restoring receiver orthogonality and lowering spectrum power.

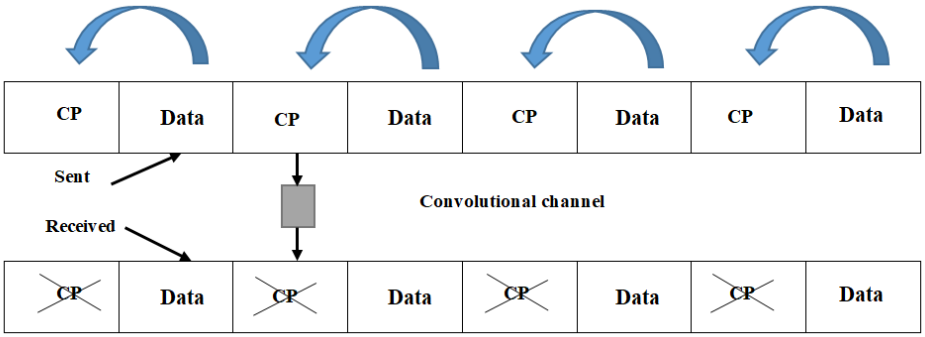

Figure 5. Cyclic prefix removal from data

As a result, as illustrated in Figure 5, shows that the receiver maintained a constant stream of data, CP elimination is crucial during demodulating. the CP length is shortened to enhance functionality and make removal easier. Consequently, the FFT deals with the received signal in the frequency domain, and the Frequency Domain Equaliser, which is based on the banded-matrix approximation technique, is introduced on the receiver side with no time lag. As an outcome, the frequency offset is computed, and the orthogonality of the waves is maintained.

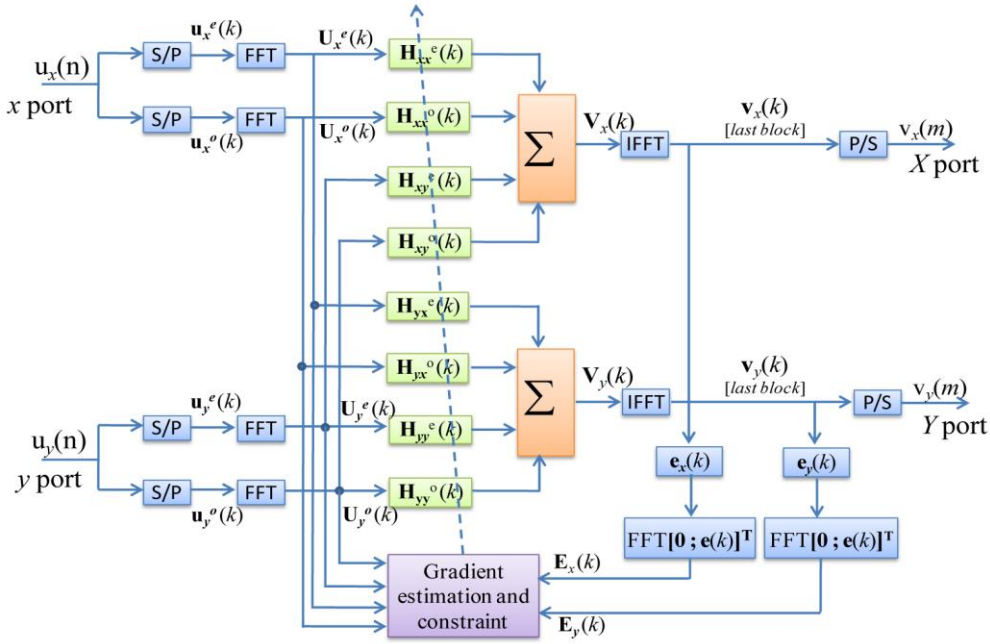

Figure 6. The suggested FDE is depicted in this diagram

In Figure 6, the first, even and odd sequences from the input sequences $u_{x,y}(n)$ are separated. Instead of processing time domain data samples by samples, the FDE handles blocks of data at a time. The length of the even and odd sequences in a block should be set to L. The modulated output signal was given for the kth block, where$u_{x,y}^{e,0}(k)$ represents a column vector of the length L, $V_x(k)$ and $E_x(k)$.

The overlap saves or overlap-add methods can be used to quickly construct linear convolution in the frequency domain; we opt for the former because it is less difficult. Additionally, we selected a percent overlap since it enables the most effective implementation. The frequency-domain input vector for subequalisers can be represented as and contains L samples from the present block and L samples from the prior block using the percent overlapping factor.

$$\mathrm{u}_{\mathrm{x,y}}^{\mathrm{e,0}}(\mathrm{k}) = \mathrm{FFT}\,[\mathrm{u}_{\mathrm{xy}}^{\mathrm{e,0}}(\mathrm{kL}-\mathrm{L}) \ldots . \mathrm{u}_{\mathrm{xy}}^{\mathrm{e,0}}(\mathrm{kL}+\mathrm{L}-1)]^{\mathrm{T}} \quad (19)$$

After padding the L tap weights of the equalisers with an equal number of zeros, a 2L-point FFT is performed. Let $H_{pq}^{e,0}(k)$ be the Zero padded tap weight vector's FFT coefficient vector $h_{pq}^{e,0}(k)$.

The gradient vector is constrained in the aforementioned equations (19), ensuring that frequency-domain tap weights are equal to their time-domain equivalents. However, each gradient limitation requires further FFT and IFFT. As long as the input sequence complies with the requirements, the complexity of the equaliser is reduced when the gradient restriction is lifted; however, when using an unconstrained FDE method, tap-weight vectors do not converge to the Wiener solution as the number of block iterations approaches infinity.

$$\mathrm{H}_{\mathrm{pq}}^{\mathrm{e,0}}(\mathrm{k}) = \mathrm{FFT}[\mathrm{h}_{\mathrm{pq}}^{\mathrm{e,0}}(\mathrm{k}), \mathrm{o}_{\mathrm{L}}]^{\mathrm{T}} \quad (20)$$

To obtain the output vector in the time domain with a column length of L, inverse FFT is used. (IFFT). Finally, the gradient decent approach is used to update tap weights in the frequency domain.

$$\mathrm{H}_{\mathrm{pq}}^{\mathrm{e,0}}(\mathrm{k}+1) = \mathrm{H}_{\mathrm{pq}}^{\mathrm{e,0}}(\mathrm{k}) + \mu\mathrm{FFT}[\nabla_{\mathrm{pq}}^{\mathrm{e,0}}(\mathrm{k}), \mathrm{o}_{\mathrm{L}}]^{\mathrm{T}} \quad (21)$$

where $\nabla_{pq}^{e,0}(k)$ is enhanced with L zeros, μ is the step-size parameter, and is the gradient vector. The output of the preceding process is fed into the demapper, which determines the signal's conjugation before using a generic QPSK demodulator and an integer to bit converter.

Thus, the frequency offset is deduced and the orthogonality of the waves was preserved. Finally, the transmitted data vectors are restored using a de-mapping method and a multiplexer block. Thus the proposed OFDM carriers all the signal and transmits and receives with low out-of-band, carrier frequency offset in an efficient and equalised manner without any error and losses. Hence, the simulation outputs are explained in the next section.

4. Result and discussion

This section includes a full discussion of the implementation outcomes as well as the proposed system's performance, as well as a comparison section to check that the proposed system is effective.

4.1. Experimental Setup

The following system specification was used to implement this work on the Matlab working platform, and the simulation results are given below,

Platform	**: MATLAB**
OS	**:** Windows 7
Processor	**:** 64-bit Intel processor
RAM	**:** 8GB RAM

4.2. Simulation Outputs

This section presents the simulation outputs and its discussion in detail upon Optimised MIMO based enhanced OFDM for Multi carrier system.

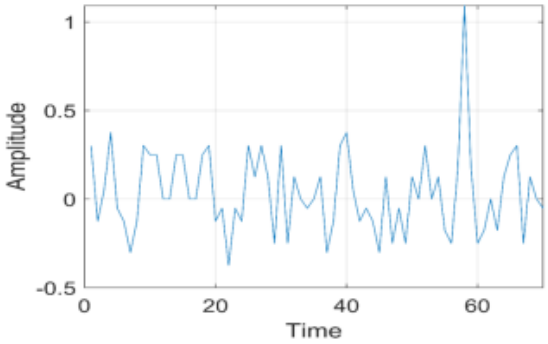

Figure 7. OFDM subcarrier indices

Figure 7 shown as each carrier's spectrum contains a null at each of the other carrier center frequency, showing that the sub-carriers are orthogonal. As a result, the carriers do not interfere with each other, allowing them to be as close together as possible in theory. As a result of the orthogonality, simultaneous transmission on a high number of sub-carriers in a short frequency range is possible without interfering with one another on the transmitter side, as shown in eqn 1. In addition, carriers in traditional FDM systems cannot overlap; hence a guard band is provided between each carrier to prevent inter-carrier interference.

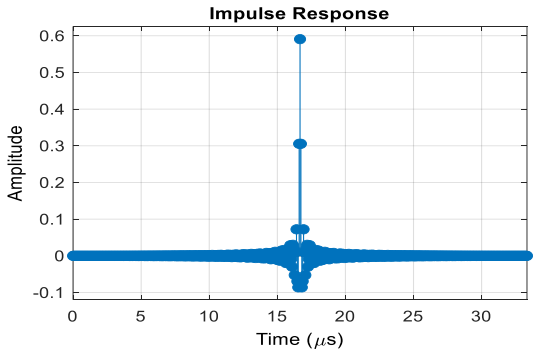

Figure 8. Impulse response

Figure 8 shows the designed filter's base-band impulse response with a bandwidth of 3 RBs. Derived from eqn (22)

$$[h, t] = \text{Impz}(b, a) \tag{22}$$

The impulse response of the model with numerator coefficients b and denominator coefficients an is denoted by this symbol. The number of samples is chosen by the function, which then provides the response coefficients in h and the sample times in t. Here, the filter's energy is limited inside the CP length, and as a consequence, the induced ISI is quite low. Later, using the proposed block-error-rate (BLER) results OFDMA (orthogonal frequency multiple access) asynchronous scheme, it is also worth mentioning that even more energy will be contained by the designed filter.

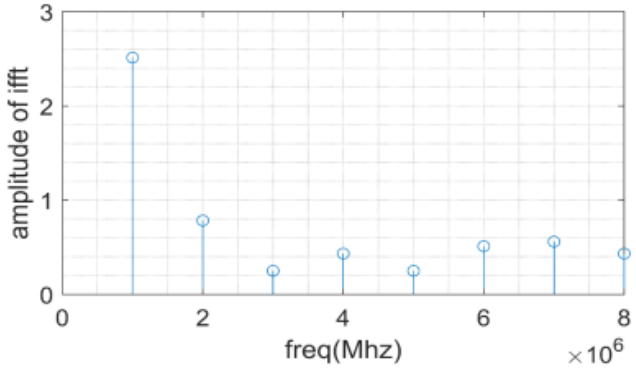

Figure 9. Amplitude of Inverse Fast Fourier transform

Figure 9 shows the IFFT amplitude is 2.8V at 1MHz, 0.9V at 2MHz, and 0.5V at 7MHz. The superimposed modulated signal onto different sub-carriers is depicted in Figure 7 calculated from eqn (1). The application of IFFT on these sub-carriers transforms complicated data symbols into Time Domain OFDM symbols, converting them from frequency to time domain.

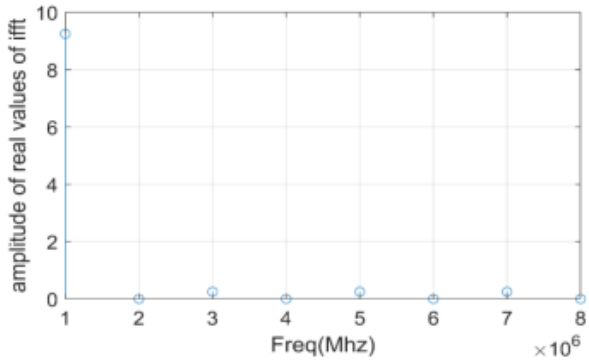

Figure 10. Amplitude of real values of IFFT

Figure 10 shows the consequence of adding the cyclic prefix to the sub-carriers. Hence, the frequency axis is the same as the two-sided power spectrum's axis. Also, the number of points in the time-domain signal determines the IFFT amplitude from eqn (5). At 3MHz of frequency, the amplitude of real values of IFFT is 0.2V. At 5MHz of frequency, the amplitude is 0.35V. At 8MHz of frequency, the amplitude is 0V.

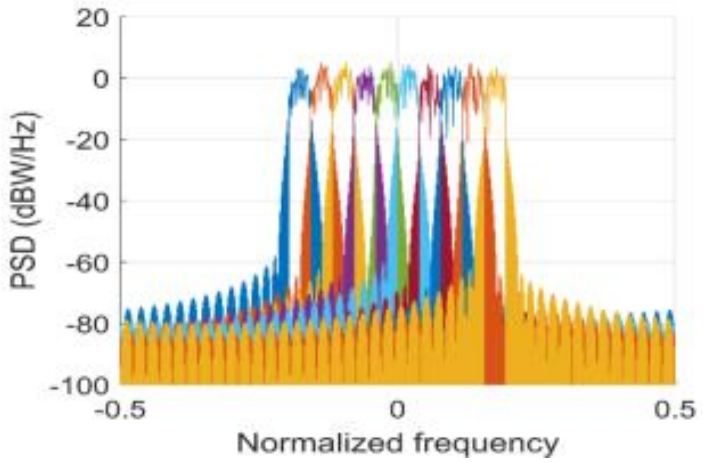

Figure 11. OFDM signal multicarriers

Figure 11 describes each carrier's spectrum has a null at the centre frequency of every other carrier in the system because the sub-carriers are orthogonal using the Multi carrier interference reduction method. Where orthogonality allows simultaneous transmission of a high number of sub-carriers in a short frequency band without interfering with each other. As a result, traditional FDM systems do not allow carriers to overlap; instead, a guard band is provided between each carrier to prevent inter-carrier interference.

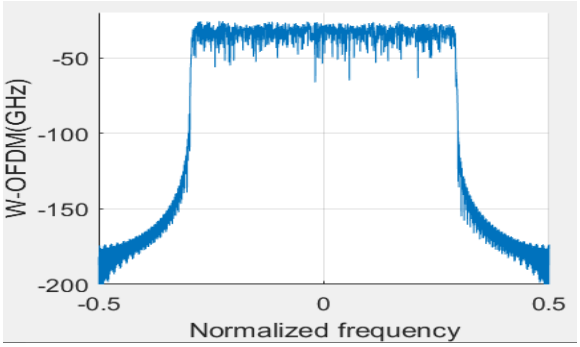

Figure 12. Normalised frequency Vs. W-OFDM(GHz)

Figure 12 shows the sub-band CP-OFDM signal is processed through a specified filter in F-OFDM. Here, only a few subcarriers at the edge are impacted since the filter's passband corresponds to the signal's bandwidth. For F-OFDM, one crucial component is that the filter length can be permitted to surpass the cyclic prefix length. Because of the filter's windowing design, inter-symbol interference is kept to a minimum (with soft truncation).

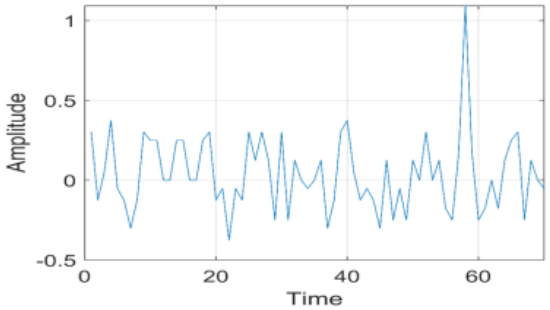

Figure 13. Source Extracted Optimised MIMO-OFDM signal

In Figure 13 is shown as the Sub-Carriers are orthogonal, and each carrier's spectrum contains a null at the system's center frequency. Furthermore, orthogonality allows for simultaneous transmission of a high number of sub-carriers in a short frequency range without interfering with each other. As a result, we can simply extract the various subcarriers on the receiver side. Traditional FDM (Frequency division multiplexing) systems, on the other hand, do not allow carriers to overlap; A guard band is provided between each carrier to prevent inter-carrier interference.

4.3. Comparison Analysis

In this section, various performances of the proposed optimised MIMO based enhanced OFDM for Multi-carrier system with 5G Waveforms have been compared with the existing models to ensure the performance of the proposed model. The evaluation metrics such as Loss, SNR(dB), Throughput (Mbits/sec), and MSE(dB) were compared with the existing models such as SimNet (2MB,1MB, and 250KB).

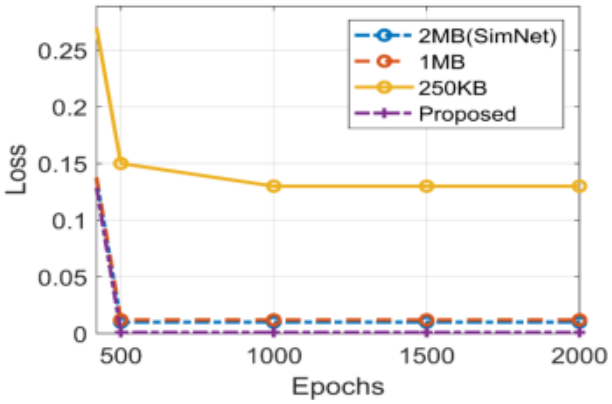

Figure 14. Epochs Vs. Loss

Figure 14 shows that the lower model size and faster convergence time for the same number of training epochs demonstrate that channel estimation and signal recognition performance are not improved. As a result, we found that using the [24] model size for SimNet training is appropriate, since it enables proper neural network training without causing overfitting. Losses are 0.02 for the proposed approach, which is 0.13 less than 250Kb at the 500th epoch. In this Table 1 analysis, the Epochs values with the Loss metric values.

Table 1. Loss

Epochs	2MB(SimNet)	1MB	250KB	Proposed
0	0.8	0.8	0.27	0.8
500	0.01	0.012	0.15	0.001
1000	0.01	0.012	0.13	0.001
1500	0.01	0.012	0.13	0.001
2000	0.01	0.012	0.13	0.001

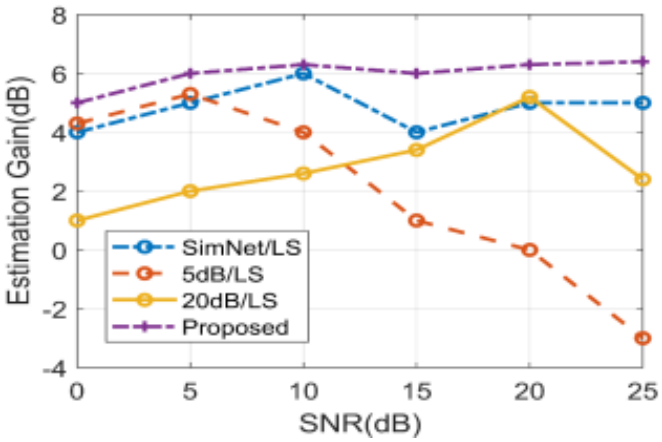

Figure 15. SNR (dB) Vs. Estimation gain

Figure 15 describes SimNet contains two sets of learnt parameters with high and low SNR, the estimate gain may be maintained above 4 dB when SNR varies from 0 to 25 dB. The estimation gain [24] will be lower if the training SNR is lower than the real SNR, and worse if the training SNR is higher than the real SNR, even though MSE can still be reduced.

Table 2 analyses the different values of Signal to Noise Ratio(dB) with the metrics of Estimation gain(dB)values.

Table 2. Estimation Gain (dB)

SNR(dB)	SimNet/LS	5dB/LS	20dB/LS	Proposed
0	4	4.3	1	5
5	5	5.3	2	6
10	6	4	2.6	6.3
15	4	1	3.4	6
20	5	0	5.2	6.3
25	5	-3	2.4	6.4

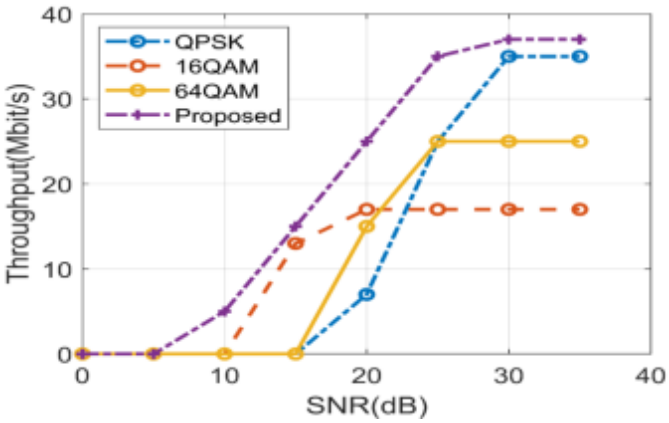

Figure 16. Throughput (Mbit/s)

Figure 16 shows performance of the Throughput Vs SNR for the Optimised MIMO-based enhanced OFDM for Multi-carrier system can provide a large improvement in throughput at a given SNR, because higher throughput modes can be employed at much lower SNR values. Hence, the optimised MIMO-OFDM was compared to Zerrouki, Hadj, et al. (2010) existing models and statistically given in Table.3. It is clear from the graph that throughput would perform better in the optimized MIMO-based enhanced OFDM than other techniques based on 16QAM, 64QAM, and QPSK; however, our proposed achieves 37 Mbit/s, which is 2 Mbit/s higher than QPSK, 12 Mbit/s higher than 64QAM. In this Table 3 evaluates the comparison of Throughput (Mb/s) in different Signal to Noise Ratio(dB)values.

Table 3. Comparison of Throughput (Mbit/s)

SNR(dB)	QPSK,1/2	16QAM,1/2	64QAM,3/4	Proposed
0	0	0	0	0
5	0	0	0	0
10	0	0	0	5
15	0	13	0	15
20	7	17	15	25
25	25	17	25	35
30	35	17	25	37
35	35	17	25	37

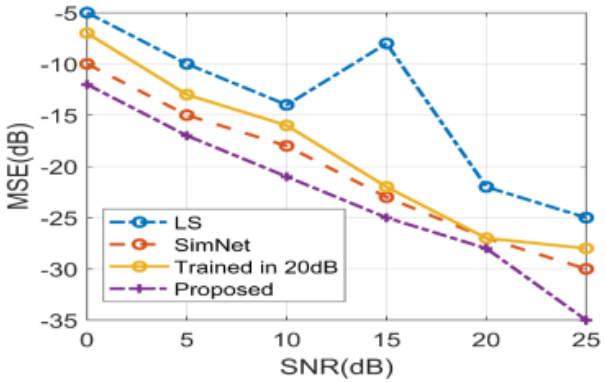

Figure 17. MSE (dB)

Figure 17 shows the estimation results in several cases. Also, SimNet achieves lower MSE in every simulated SNR (Signal to Noise ratio) when compared to LS (Least squares). The FC-DNN trained in a 5dB environment performs worse than the LS when the SNR is over 20dB, whereas the training output in a 25dB environment performs poorly when the SNR is high (Bao, Yicheng et al., 2020). In other words, an FC-DNN (fully connected-deep neural network) trained in low SNR situations has a negative impact on channel estimation in high SNR environments. The suggested SimNet is able to predict the channel situation with accuracy when the CP is removed, allowing transmission power to be saved. In Table 4, the comparison of Mean Square Error(dB) with different Signal to Noise Ratio(dB) values is shown.

Table 4. Comparison of MSE (dB)

SNR(dB)	LS	SimNet	Trained in 20dB	Proposed
0	-5	-10	-7	-12
5	-10	-15	-13	-17
10	-14	-18	-16	-21
15	-8	-23	-22	-25
20	-22	-27	-27	-28
25	-25	-30	-28	-35

5. Conclusions

OFDM is a very desirable wireless communication method, because of its spectrum efficiency and channel longevity. MIMO technology has been identified to substantially boost the capacity and performance of a wireless system. Optimised MIMO-OFDM is a spectrally localised multicarrier waveform that can achieve optimum frequency localisation while keeping the benefits of the Cyclic prefix OFDM. This was accomplished by allowing the filter length to exceed the OFDM cyclic prefix length and constructing the filter appropriately. The SNR conditions in which it is trained are 10dB and 25dB.As a consequence, in terms of channel estimate on performance, it has a lower MSE over a large SNR range than other training strategies. Finally, the signal detection results show that the proposed optimised MIMO-based enhanced OFDM for multi-carrier systems with 5G waveforms has a BER similar to deep neural networks and may increase detection performance even when clipping distortion is prevalent. This study suggests a quick and precise way to estimate the channel in a MIMO-OFDM system that has been optimised, and it justifies more study and development.

REFERENCES

[1] **Ahmed, S.R., Abdullah, A.S., Hammash, N.M. (2020),** ***Universal Filtered Multicarrier (UFMC) vs. Orthogonal Frequency Division Multiplexing (OFDM).*** In *Journal of Physics: Conference Series, IOP Publishing, 1530*(1), 012092;

[2] **Alrubaee, S.H., Ismail, M., Altahrawi, M.A., Burhan, B.B. (2020),** ***Filter Bank Multi-Carrier Modulation Technique for Vehicle-to-Vehicle Communication.*** *Journal of Communications., 15*(7), 566-571;

[3] **Attar, H.H., Solyman, A.A., Abd-Elnaser Fawzy, M., Khosravi, M.R., Menon, V.G., Bashir, A.K., Tavallali, P. (2020),** ***Efficient equalisers for OFDM and DFrFT-OCDM multicarrier systems in mobile E-health video broadcasting with machine learning perspectives.*** *Physical Communication, 42*, 101173;

[4] **Bao, Y., Tan, Z., Sun, H., Jiang, Z. (2020),** ***SimNet: Simplified deep neural networks for OFDM channel estimation.*** *2020 IEEE 3rd International Conference on Information Communication and Signal Processing (ICICSP). IEEE*;

[5] **Chen, Q., Li, L. (2021),** ***A Deep Learning Based Equalization Scheme for Bandwidth-compressed Non-orthogonal Multicarrier Communication.*** *Journal of Internet Technology, 22*(5), 1001-1009;

[6] **Dang, S., Zhou, J., Shihada, B., Alouini, M.S. (2020),** ***Relay assisted OFDM with subcarrier number modulation in multi-hop cooperative networks.*** *IEEE Wireless Communications Letters, 9*(11), 1869-1873;

[7] **Hou, J., Wei, W., Yang, Z., Xinyi, L., Ying, X. (2020),** ***Multi-objective quantum inspired evolutionary SLM scheme for PAPR reduction in multi-carrier modulation.*** *IEEE Access, 8,* 26022-26029;

[8] **Jiang, L., Zhang, H., Cheng, S., Lv, H., Li, P. (2020),** ***An overview of FIR filter design in future multicarrier communication systems.*** *Electronics, 9*(4), 599;

[9] **Le, H.A., Van Chien, T., Nguyen, T.H., Choo, H., Nguyen, V.D. (2021),** ***Machine Learning-Based 5G-and-Beyond Channel Estimation for MIMO-OFDM Communication Systems.*** *Sensors, 201*(14), 4861;

[10] **Liu, X., Xu, T., Darwazeh, I. (2020),** ***Coexistence of orthogonal and non-orthogonal multicarrier signals in beyond 5G scenarios.*** *2020 2nd 6G Wireless Summit (6G SUMMIT). IEEE*;

[11] **Mattera, D., Tanda, M., Bellanger, M. (2021),** ***Comparing the performance of OFDM and FBMC multicarrier systems in doubly-dispersive wireless channels.*** *Signal Processing, 179,* 107818;

[12] **Murad, M., Tasadduq, I.A., Otero, P. (2020),** ***Towards multicarrier waveforms beyond OFDM: performance analysis of GFDM modulation for underwater acoustic channels.*** *IEEE Access, 8,* 222782-222799;

[13] **Niu, Z., et al. (2020),** ***The research on 220GHz multicarrier high-speed communication system.*** *China Communications, 17*(3), 131-139;

[14] **Park, M.C., Dong, S.H. (2021),** ***Deep Learning-Based Automatic Modulation Classification With Blind OFDM Parameter Estimation.*** *IEEE Access, 9,* 108305-108317;

[15] **Sarowa, S., Kumar, N., Agrawal, S., Sohi, B.S. (2020),** ***Evolution of PAPR reduction techniques: A wavelet based OFDM approach.*** *Wireless Personal Communications, 115*(2), 1565-1588;

[16] **Shaikhah, S.K., Mustafa, S. (2020),** ***A robust filter bank multicarrier system as a candidate for 5G.*** *Physical Communication, 43,* 101228;

[17] **Shi, C., Wang, Y., Wang, F., Salous, S., Zhou, J. (2020),** ***Joint optimization scheme for subcarrier selection and power allocation in multicarrier dual-function radar-communication system.*** *IEEE Systems Journal, 15*(1), 947-958;

[18] **Srivastava, M.K., Shukla, M.K., Srivastava, N., Shankhwar, A.K. (2020),** ***A hybrid scheme for low PAPR in filter bank multi carrier modulation.*** W*ireless Personal Communications, 113*(2), 1009-1028;

[19] **Wang, X., ten Brink, S. (2020),** ***SINR Analysis of Different OFDM-Inspired Waveforms Over Doubly Dispersive Channels.*** *IEEE Transactions on Vehicular Technology, 69*(9), 9459-9468;

[20] **Wang, Y., Shi, Z., Ma, X., Liu, L. (2021),** ***A Joint Sonar-Communication System Based on Multicarrier Waveforms.*** *IEEE Signal Processing Letters*;

[21] **Zerrouki, H., Feham, M. (2010),** ***High Throughput of Wimax Mimo Ofdm Including Adaptive Modulation and Coding***. arXiv preprint arXiv:1002.1954.